Use of Surface Data to Estimate Geostrophic Transport

ANANDA PASCUAL AND DAMIÀ GOMIS

Departament de Física, Universitat de les Illes Balears, and Institut Mediterrani d'Estudis Avançats, IMEDEA (CSIC-UIB), Palma de Mallorca, Spain

(Manuscript received 31 October 2001, in final form 27 November 2002)

ABSTRACT

An extension of the use of altimetric data aimed at inferring the vertical structure of the geostrophic velocity field (and thereby to compute transports) is explored. The method is based on the assumption that altimetry provides a reliable measure of dynamic height (DH), and on the fact that DH and the density field can both be expressed in terms of the DH empirical orthogonal functions (EOFs). It is then argued that when altimetry is complemented by surface density data, it is possible to determine the amplitudes of the two leading EOFs of the mass field, which altogether usually account for a large percentage of the field variance.

The method is tested in the western Mediterranean, where historical databases contain enough data as to compute statistically significant EOFs. Results indicate that with altimetric data alone (i.e., DH in the tests), the EOF-based method can estimate the actual velocity field with an uncertainty of about 60% (in terms of total transport). However, if surface density is also available, estimates have an uncertainty of only 20%. Limitations of the method such as the underlying statistical assumptions, data errors, and the assumed equivalence between altimetry and DH are also discussed.

1. Introduction

Satellite altimetry is a powerful tool providing periodic synoptic measurements of the sea surface height along tracks. Unfortunately, altimetric observations alone do not give any direct subsurface information.

Different strategies aimed at estimating subsurface temperature or velocity from altimetric height have been developed. Carton and Katz (1990) estimated the seasonal transport in the North Atlantic Equatorial Countercurrent assuming a very simple two-layer model. Other methods are based on dynamical models (Hurlburt 1984). Some simple linear fits have been used for inferring subsurface temperature and transport from TOPEX/Poseidon (hereafter T/P) data (Gilson et al. 1998; Imawaki et al. 1997). In the studies of altimetric data assimilation into numerical models these types of statistical regressions have also been applied (e.g., Mellor and Ezer 1991; Ezer and Mellor 1994; Oschlies and Willebrand 1996). However, vertical empirical orthogonal functions (EOFs) have been shown to be a very efficient tool in reducing degrees of freedom of a dataset (Gavart and de Mey 1997). Carnes et al. (1990) derived synthetic temperature profiles from an empirical relationship between sea surface height and the amplitudes of the EOFs of the vertical structure of temperature in the Gulf Stream region. De Mey and Robinson (1987) and more recently Gavart et al. (1999) performed a vertical projection of surface data in a vertical subspace given by an EOF and this was implemented into an assimilation scheme.

In this work we propose and investigate a new method for propagating the information measured at surface into the body of the ocean. It essentially consists of fitting altimetric and in situ surface observations to the empirical vertical modes of the mass field (EOFs) derived from historical hydrography. A key assumption underlying the method is that altimetric data provide a reliable measure of dynamic height (hereafter DH), and on the fact that DH and the density field can both be expressed in terms of the DH EOFs. It is then showed that when altimetry is complemented by surface density data, it is possible to determine the amplitudes of the two leading EOFs of the mass field, which altogether usually account for a large percentage of the field variance. For an intercomparison study, we have selected the technique proposed by Carnes et al. (1990) as a reference method.

The methods are tested with hydrographic data alone, evaluating the capability of inferring DH profiles from surface DH and density data. The reason for not using actual altimetry is twofold: first, because the availability of simultaneous, collocated altimetry and hydrographic data is clearly not enough to carry out statistically significant tests. Second, because in this way the differences between extrapolated and actual profiles will be due exclusively to the limitations of the methods themselves, and not to inadequacies in the data.

Corresponding author address: Dr. Ananda Pascual, Institut Mediterrani d'Estudis Avançats (CSIC-UIB), Grup d'Oceanografia Interdisciplinar, C/Miquel Marquès, 21, 07190 Esporles, Mallorca, Spain. E-mail: ananda.pascual@uib.

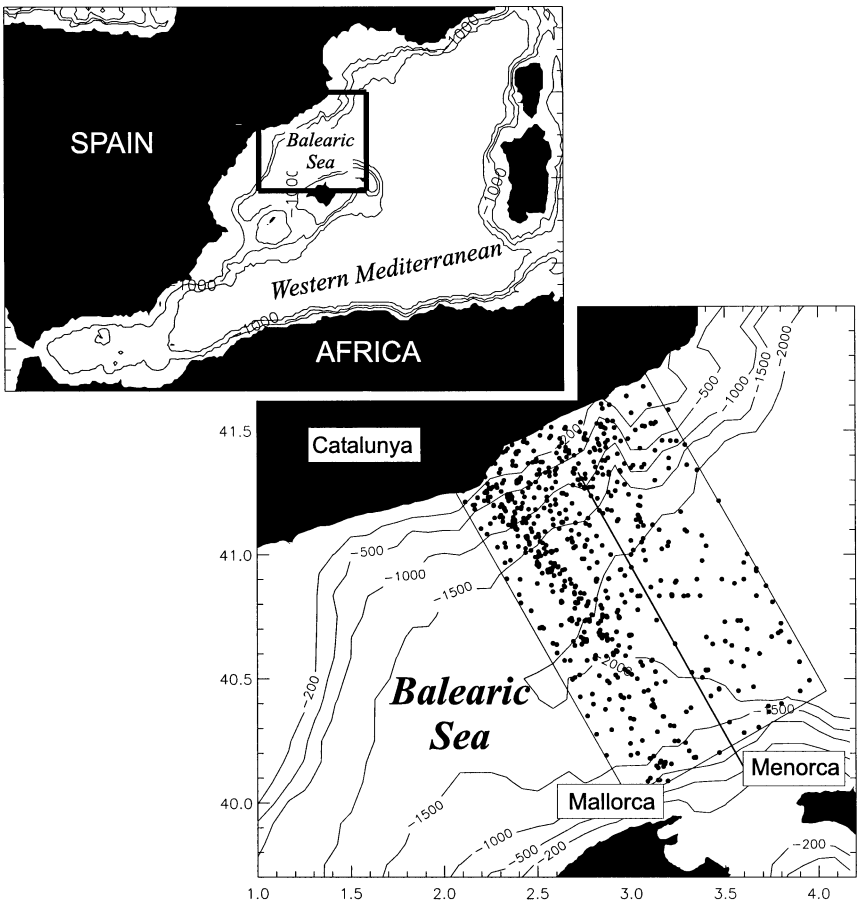

FIG. 1. Location map of the Balearic Sea, with the domain selected to test the extrapolation methods. Dots correspond to the position of available historical hydrographic stations. The continuous line crossing the domain is T/P track 70.

The region selected for the application of the methods is the Balearic Sea (western Mediterranean; Fig. 1), where some altimeter tracks run almost perpendicular to the main currents. Furthermore, several authors (e.g., Font et al. 1995) have pointed out the importance of an accurate computation of the current transports in the Balearic Sea for a correct modeling of the circulation in the different sub-basins of the western Mediterranean. Nevertheless, the applicability of the methods is well beyond the particular region studied in this work. The only constraints are the existence of enough historical hydrographic data as to produce significant statistics (i.e., to yield significant EOFs), and that the ocean have considerable variability with respect to the accuracy of altimetry.

The paper is organized as follows. In section 2 we explain the statistical basis underlying the proposed vertical extrapolation method and also review an alternative technique that will be used as a reference method. The application of the methods to the Balearic Sea is presented in section 3. This begins with a short background on the regional dynamics and a description of the dataset and the data preprocessing. Results are presented showing examples from two particular cruises and then summarizing the statistics obtained from the whole independent datasets submitted to the tests. Finally, in section 4 we discuss the general limitations of the methods and the feasibility of the methods for an operational application.

2. Extrapolation methodology

Empirical orthogonal functions have been frequently used to study temporal and spatial patterns in geophysical data (e.g., Pedder and Gomis 1998; Leuliette and Wahr 1999, among many others). The reason is that they provide the most efficient (in terms of accounted variability) decomposition of the data into orthogonal modes. The use of EOFs to estimate the deep-ocean structure from upper-ocean observations is also not new. Haney et al. (1995) tested an empirical method in which the EOFs amplitudes were obtained using sequential fits. That study illustrates the accuracy of the extrapolation over an increasing depth, but always assuming that observations covered at least the upper 100 m. With the same purpose, Boyd et al. (1994) used a least squares

minimization technique. Closer to our work, Carnes et al. (1990) used EOFs to extrapolate altimetric data downward. This technique, chosen as a reference in order to evaluate the goodness of the method proposed in this work, will be described later on.

a. EOF computation

The theory behind EOF computation is described in several works (see, e.g., Boyd et al. 1994). For a certain variable ϕ, let $\phi_{x,y}(p)$ represent a collection of profiles located at (x, y) and reporting data at a number P of common pressure levels. The first step is the computation of anomaly profiles $\phi'_{x,y}(p)$ by subtracting the mean historical profile $[\overline{\phi}(p)]$ from each of the observed profiles. The $(P \times P)$ level-covariance matrix is then constructed from anomaly profiles and diagonalized. Because it is a real, symmetric positive-definite matrix, the set of eigenvectors (the EOFs) forms an orthogonal basis of the P-vector space, and the eigenvalues are real and positive. The ratio of each eigenvalue to the trace (the sum of all eigenvalues) yields the fraction of field variance explained by the corresponding EOF.

Any anomaly profile (not only those used to compute the EOFs) can therefore be expressed as a linear combination of the P EOFs. [The coefficients (or amplitudes) can be determined simply as the scalar product of the profile by each of the EOFs.] However, a reduced number N ($\ll P$) of leading (in terms of explained variance) EOFs is usually enough to account for most of the field variance (e.g., the part of the field that cannot be attributed to ''noise,'' according to some prescribed model). Denoting the ''modeled'' anomaly profiles as $\hat{\phi}_{x,y}(p)$, they can be expressed as

$$\hat{\phi}_{x,y}(p) = \sum_{i=1}^{N} A_i(x, y)\mathrm{EOF}_i(p), \tag{1}$$

where $\mathrm{EOF}_i(p)$ are the eigenvectors or EOFs and $A_i(x, y)$ are the coefficients or EOF amplitudes. It is worth noting that, in general, the historical profiles used to compute the EOFs are from different locations and at different times, contributing, both temporal and spatial variability in a combined way (no distinction).

b. Estimation of the amplitudes

The problem being considered here is that of reconstructing a whole profile when only the upper part is available. Assuming, as in (1), that only the first N leading EOFs are significant, this yields a linear equation with the same N unknowns (the N amplitudes) for each profile level. Therefore, it turns out that for the amplitudes to be determined it is enough that data are available at N levels of the profile. (In this sense, EOFs must be regarded as a useful technique to reduce the degrees of freedom of a dataset.) Once the amplitudes are determined, the missing levels can be reconstructed by simply operating the amplitudes onto the whole vertical extension of the EOFs.

Now consider a problem of obvious relevance for almost any kind of satellite data: the possibility of reconstructing profiles when only surface (i.e., one level) data are available. According to the previous statements, this would only be possible when a single vertical mode accounts for most of the field variance. This is, when modeled anomaly profiles can be expressed as

$$\hat{\Phi}_{x,y}(p) = A_1^{\Phi}(x, y)\mathrm{EOF}_1^{\Phi}(p). \tag{2}$$

In this case, obtaining the single amplitude corresponding to each profile $A_1(x, y)$ would be straightforward given the surface data $[\hat{\Phi}_{x,y}(p_0)]$ and the surface component of the leading EOF $[\mathrm{EOF}_1(p_0)]$. Assuming that altimetry provides a reliable measure of surface DH, and provided that available historical DH profiles are enough as to compute statistically significant EOFs, this would imply the possibility of reconstructing DH profiles (and therefore geostrophic velocity and transport along the whole water column) from altimetric data alone.

The main objection to the previous approach is that the field variability is usually not accounted for by a single EOF. In terms of dynamics, this would imply having an equivalent barotropic ocean, which is characterized by the absence of any vertical tilting in the mass field (i.e., a mass field where density and DH contours are the same). Although this can be the case for some basins (see section 4), it is far from being true in general.

It can be argued that although more than one EOF is required to describe the anomaly field, (2) will still allow one to determine the amplitude of the first leading EOF, so that at least a significant part of the profile variance is recovered. However, for this to be correct, only the fraction of the observed surface variance actually explained by the first EOF (and not actual surface observations) should be quoted in the left member of (2). Nevertheless, because the method proposed in the following is somehow an extension of this first method (hereafter referred to as the 1-EOF method), the capability of (2) to reconstruct DH profiles will also be tested in the intercomparison study.

c. The proposed method

A feature of the EOF decomposition (1) worth noting is that the horizontal and vertical dependence of the modeled anomaly field appear in separate terms: the EOFs account for the vertical dependence, whereas the amplitudes account for the horizontal dependence. This is particularly relevant when two distinct variables are related by a linear operator involving either only the horizontal or only the vertical dimension. In the first case (e.g., for DH and geostrophic velocity), the two variables would share the same EOFs and the amplitudes

would be related by the linear operator linking the variables.

In the second case (more relevant to this work), the two variables can be expressed in terms of vertical modes that are related by the linear operator linking the variables. But most important, the amplitudes of the modes would be the same for both variables. This is the case for DH (denoted by Φ) and specific volume (α), since the former is obtained as the vertical integration of the latter:

$$\Phi_{x,y}(p) = -\int_{\text{pref}}^{p} \alpha_{x,y}(p')\, dp' \Rightarrow \alpha_{x,y}(p) = -\frac{\partial \Phi_{x,y}(p)}{\partial p}. \tag{3}$$

Therefore, specific volume profiles can be decomposed in such a way that the coefficients (amplitudes) are the same as for DH (hereafter denoted by A_i^{Φ}):

$$\hat{\alpha}_{x,y}(p) = -\frac{\partial \hat{\Phi}_{x,y}(p)}{\partial p} = -\sum_{i=1}^{N} A_i^{\Phi}(x, y)\frac{\partial \text{EOF}_i^{\Phi}(p)}{\partial p}. \tag{4}$$

This implies that if both types of surface data (Φ and α) are available, then it will be possible to compute the amplitudes of the two leading DH modes by solving the linear equation system:

$$\hat{\Phi}_{x,y}(p_0) = A_1^{\Phi}(x, y)\text{EOF}_1^{\Phi}(p_0) + A_2^{\Phi}(x, y)\text{EOF}_2^{\Phi}(p_0)$$

$$\hat{\alpha}_{x,y}(p_0) = -A_1^{\Phi}(x, y)\frac{\partial \text{EOF}_1^{\Phi}(p)}{\partial p}\bigg|_{p_0} - A_2^{\Phi}(x, y)\frac{\partial \text{EOF}_2^{\Phi}(p)}{\partial p}\bigg|_{p_0}. \tag{5}$$

Again, this will be strictly correct only when two vertical DH modes account for most of the variability of the DH field. An additional limitation comes from the fact that the vertical modes used to decompose $\hat{\alpha}$ do not necessarily coincide with actual specific volume EOFs (nor are they necessarily orthogonal). In practice, however, these modes usually do account for a large fraction of the field variance. This means that altogether, the proposed method (hereafter referred to as the 2-EOF method) has a much larger potential applicability than the 1-EOF approach.

In practice, the 2-EOF method could be implemented when both sea level (assimilated to DH) and surface density data are available. The latter could come from ships of opportunity (e.g., from thermosalinographs installed in ferries running approximately along altimeter tracks). Or, in the future, from a combination of surface salinity provided by the Soil Moisture and Ocean Salinity (SMOS) satellite mission (Font et al. 1999) and sea surface temperature data from Advanced Very-High Resolution Radiometer (AVHRR) satellite imagery.

d. A reference method: Least squares fit

As stated in the introduction to this section, we selected the method proposed by Carnes et al. (1990) as a reference method for the intercomparison study. These authors used a least squares fit to derive synthetic temperature profiles from a regression relationship between sea surface height and the amplitudes of EOFs computed for the temperature field. Here, we will follow the same procedure, except that we will work with DH profiles instead of temperature profiles. Namely, the amplitudes of DH EOFs computed from the historical dataset will be fitted to surface DH using third-order polynomials:

$$A_i^{\Phi}(x, y) = b_{0i} + b_{1i}\Phi(x, y, p_0) + b_{2i}\Phi^2(x, y, p_0) + b_{3i}\Phi^3(x, y, p_0). \tag{6}$$

As for the 1-EOF and 2-EOF methods, once the amplitudes are determined they allow the retrieval of the complete DH profile. An apparent advantage of the method by Carnes et al. (1990) is that in principle it allows to determine the amplitudes of all the modes (not only the two first ones) by applying the regression given in Eq. (6). However, because this type of fitting is completely empirical (with no physical or statistical basis), it usually results in a poor correlation for high-order amplitudes.

3. Testing the methods in the Balearic Sea

The reason for testing the methods in the Balearic Sea is twofold. First, historical databases contain enough data to compute statistically significant EOFs. Second, the capability of inferring the vertical structure of DH (and therefore of the geostrophic velocity and transport) along altimetry tracks would represent a major step forward for the operational monitoring of this region. Of particular interest is T/P track number 70, which runs just along the natural northern boundary of the Balearic Sea and is oriented almost perpendicular to the main inflow and outflow of the basin (see Figs. 1 and 2).

a. Regional background

The general circulation of the Balearic Sea is fairly well known and has been described by several authors (e.g., Font et al. 1988; Pinot et al. 1995). The circulation is controlled by two well-defined currents associated with density fronts: the Catalan front over the mainland continental slope and the Balearic front, located over the insular slope (Fig. 2). The Catalan front is a shelf/slope front that separates high saline water, in the center of the Balearic Sea, from the less dense water transported by the Northern Current, fed in the Gulf of Lions and Catalan shelves by fresh continental water. The Northern Current flows southward, along the continental slope, until it either exits the basin through the Ibiza Channel or recirculates cyclonically over the islands slope forming the Balearic Current over the islands slope. This latter current is also fed by warm and fresh waters coming from the Algerian Basin through the Balearic Channels. Thus, the Balearic front separates the

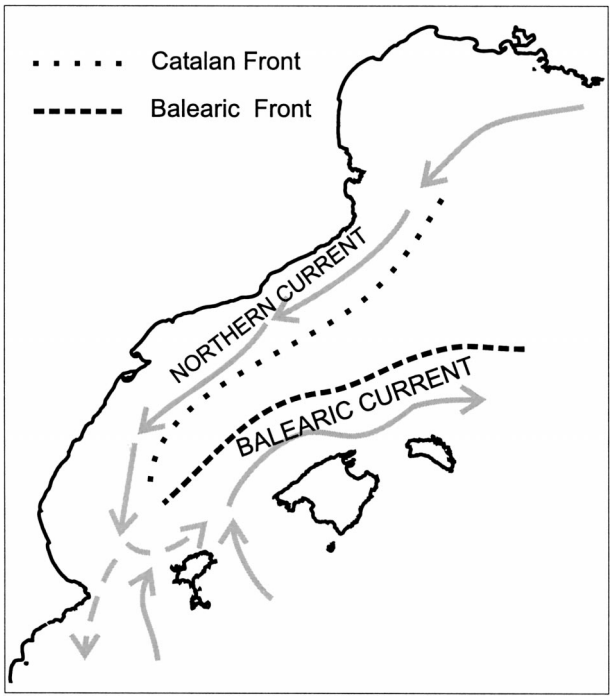

FIG. 2. Main fronts and currents in the Balearic Sea.

dense water, present in the middle of the basin, from the lighter water transported by the Balearic Current. Both currents (Northern and Balearic) have widths of the order of 50 km and represent the major forcing for the circulation, since winds have been shown to produce only transient perturbations (Font 1990).

Acoustic Doppler current profiler (ADCP) measurements of the Northern Current have shown velocities in good agreement with geostrophic velocities (typical values are of about 20–25 cm s^{-1} at surface, decreasing with depth; Castellón et al. 1990). The Balearic Current is also in good geostrophic balance with maximum surface velocities about 25–30 cm s^{-1} (Pinot et al. 1995). This is the expected behavior in a region where tidal currents are weak (a few centimeters per second) and inertial oscillations only occur after strong storms, mainly in autumn and winter (Pinot et al. 1995). Thus, the geostrophic transport from a good estimate of the dynamic height field will be a good estimate of the actual transport.

Previous in situ and satellite imagery studies (Tintoré et al. 1990; López García et al. 1994) have found that the Northern and Balearic Currents are characterized by relevant spatial and temporal variability, with a large variety of mesoscale features (meanders, eddies, and filaments) strongly interacting with the basin-scale circulation. On the seasonal timescale, observations of the Northern Current (Bethoux et al. 1988; Font et al. 1988) provide evidence of a higher transport in winter than in summer (with associated geostrophic transports of about 1.5–2 Sv and 1 Sv, respectively, where 1 Sv $\equiv 10^6$ m^3 s^{-1}), while the opposite happens for the Balearic Current (about 0.3 Sv in winter compared to 0.6 in summer). It can therefore be envisaged that one of the main applications of the method proposed in this work will be to study the complex time variability of the regional mass transport.

b. Data

1) THE DATASET

The hydrographic data used in this study have been obtained from three sources: the MEDATLAS historical database (consisting of most hydrographic data collected in the region prior 1992; see Fichaut et al. 1997), two more recent oceanographic surveys carried out in 1993 and 1995, and the climatological MODB seasonal fields (computed from the MODB database; see Brasseur et al. 1996).

Until 1982, measurements were obtained from traditional hydrographic stations with sampling bottles, reversing thermometers and manual salinity determinations. Since then, most hydrographic data have been collected by CTD casts. In order to use the maximum amount of data to produce significant statistics, both CTD and bottles were included in our dataset. The main difference between the two is that temperature and salinity profiles from bottles are only given at several depths (10 or 15 at most) from bottom to surface, in contrast to almost continuous CTD profiles. In order to make them more equivalent, bottle data were interpolated every 10 db with cubic splines (see Fig. 3 as an example).

Within the selected domain (see Fig. 1), the total amount of available stations is 853: 538 sampled in summer and 315 in winter. Here ''summer'' means the stratified season, from April to September, and ''winter'' means the more vertically homogeneous season, from October to March, as indicated by previous authors (Font et al. 1988). Of the whole set of profiles, only those reaching the reference level chosen for geostrophic computations will be used. First, because DH necessarily refers to that level, and second, because only complete profiles can be used for the EOF analysis. For a reference level of 400 m [see section 3b(2), the discussion of the reference level] there are 159 complete profiles in winter and 173 in summer. The monthly distribution of these profiles is shown in Table 1. Although there are months with a number of profiles larger than others, these are clearly not concentrated on one or two particular months. This gives some confidence on the representativeness of the seasonal division.

The whole dataset was separated into two subsets: the so-called independent and dependent datasets, respectively. The first, used to test the extrapolation methods, consisted of 15 cruises, all of them carried out between 1982 and 1995, with CTD soundings providing a good coverage of the region. The dependent dataset, that is,

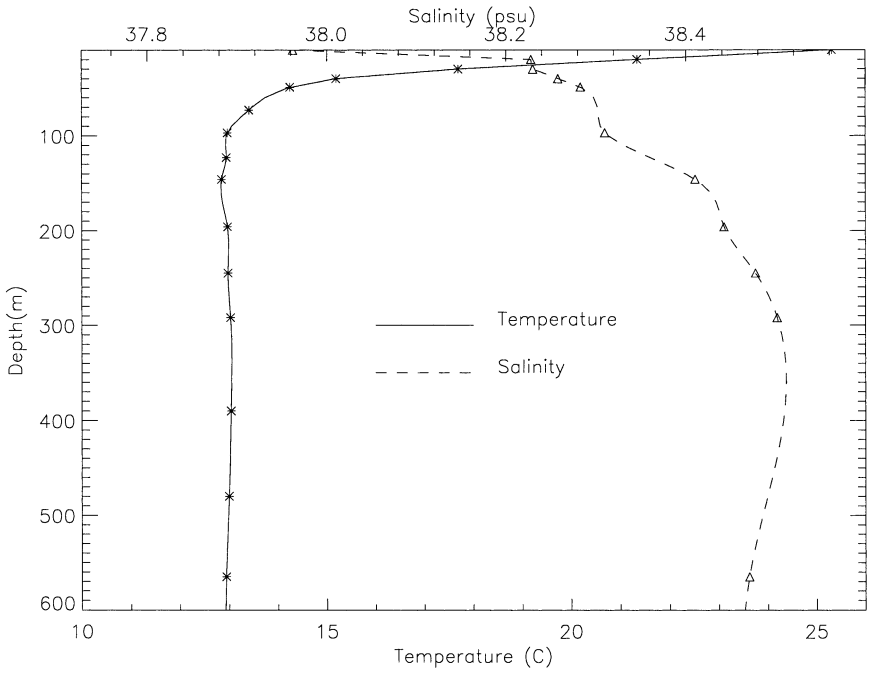

FIG. 3. Example of a bottle profile interpolated using cubic splines. Asterisks and triangles represent the original values and the continuous and dashed lines are the interpolated temperature and salinity profiles.

all historical data except the independent data, was used to compute the EOFs.

2) THE SPATIAL OBJECTIVE ANALYSIS

For a direct comparison between different datasets (e.g., hydrographic data and altimetry), some kind of horizontal interpolation is required in order to examine the fields at common spatial locations. Also, if derived variables (such as geostrophic velocity) are to be obtained from dynamic height, we need to estimate the later on a regular grid.

Thus, a spatial objective analysis was carried out for every cruise of the independent dataset. The grid covered the box selected in Fig. 1 (oriented so that a line of grid points would coincide with T/P track 70) and the separation between grid points was 3.5 km (about half of the altimeter's fingerprint). The interpolation method was a 2D successive correction scheme with weights normalized in the ''observation space'' in order to approach Optimum Statistical Interpolation (Bratseth 1986). Following previous studies dealing with mesoscale dynamics in the Mediterranean (Pinot et al. 1995), the characteristic length scale was set to 20 km. An additional normal-error filter convolution was also applied in the way proposed by Pedder (1993) in order to filter out scales that cannot be resolved by the sampling. The cutoff wavelength was set to 20 km (approximately twice the mean separation distance between stations, although the station distribution is not very homogeneous).

TABLE 1. Temporal distribution of historical hydrographic data within the selected domain (see Fig. 1). The values correspond to the number of complete profiles, that is, those reaching the reference level of 400 m and used to compute the EOFs.

Summer		Winter	
Month	No. of stations	Month	No. of stations
Apr	59	Oct	16
May	9	Nov	56
Jun	33	Dec	1
Jul	57	Jan	1
Aug	11	Feb	62
Sep	4	Mar	23

The interpolation was carried out on a set of horizontal levels spanning the vertical domain (from surface to the reference level) with a 10-db spacing. The problem of the reference level is particularly relevant to horizontal transport, since velocity differences of a few centimeters per second extending over the whole vertical domain can result in substantial transport differences. We evaluated the dependence of transport with respect to the reference level by computing the geostrophic velocity referred to a depth between 10 and 600 db (a usual reference level for studies in the Balearic Sea; e.g., Pinot et al. 1995). The resulting geostrophic transport across different sections parallel to the T/P track was then computed as a function of the reference level. The difference (in terms of transport underesti-

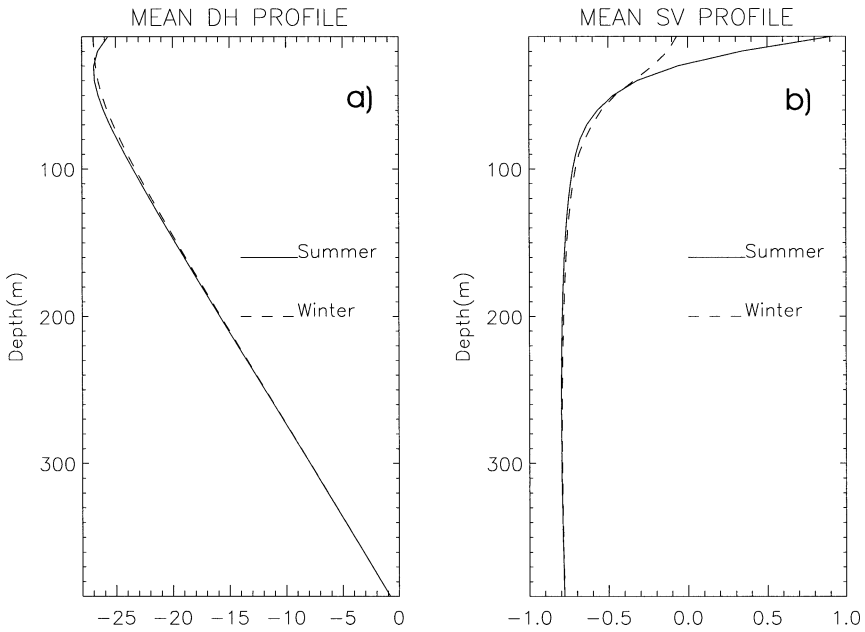

FIG. 4. (a) Dynamic height (dyn cm) mean profile for the summer and winter seasons in the Balearic Sea. (b) As in (a) but for specific volume anomaly (10^{-6} m^3 kg^{-1}).

mation) between taking the reference level at 600 db and 400 db is only about 4%, which is clearly less than the accuracy expected from any of the presented extrapolation methods. On the other hand, by using a reference level of 400 db, the amount of historical data that can be included in the computation of DH EOFs is considerably larger (from 89 to 159 profiles in winter, and from 81 to 173 in summer). We therefore selected 400 db as the geostrophic reference level.

c. EOFs in the Balearic Sea

As indicated previously, separate computations were made for the summer and winter seasons. The justification for this separation lies in the different stratification conditions observed in the region during the two seasons. Figure 4a shows the mean summer and winter DH profiles. While the mean winter profile increases monotonically with depth, the summer profile shows a sudden change of the slope in the upper 40 m. Differences are more clear when looking at the specific volume anomaly (SVAN), that is, the vertical derivative of DH (Fig. 4b). In the first 40–60 m, SVAN is positive in summer, while in winter it is negative at all depths (SVAN is negative when the density of the water being sampled is higher than the density of a standard water mass defined with $T = 0$°C and $S = 35$ psu). Although the stratification of upper levels is substantially weaker in winter than in summer, it is difficult to define an actual mixed layer in the mean profile. This is due to averaging over many profiles, with each of them having a marked mixed layer but not all of them at the same depth (it actually ranges between 20 and 50 m). However, there are also a few profiles, corresponding mainly to autumn (October and November) that do not present a mixed layer (the absence of strong winds can increase the stratification).

TABLE 2. Percentage of variance accounted by the five leading seasonal EOFs of dynamic height in the Balearic Sea.

	Summer	Winter
EOF 1	79.64	79.26
EOF 2	18.24	18.78
EOF 3	1.45	1.38
EOF 4	0.44	0.42
EOF 5	0.12	0.08
Accumulated	99.89	99.92

The variance explained by each of the five leading EOFs is presented in Table 2, and it is approximately the same for both seasons. The first DH EOF accounts for about 79% of the total variance and the second one accounts for about 18% (making a total of 97%). Therefore, although the first mode is clearly dominant, the second mode is not negligible at all. In order to evaluate the significance of the modes we followed the method proposed by Overland and Preisendorfer (1982). Results indicated that the two first modes are clearly significant, while the others could not be distinguished from those obtained from series of white noise.

Regarding the shape of the two DH leading modes (Fig. 5), it is similar for both seasons. The interpretation of these shapes is not always obvious, since there is not a necessary correspondence between the empirical modes and dynamical or hydrographic features. Because

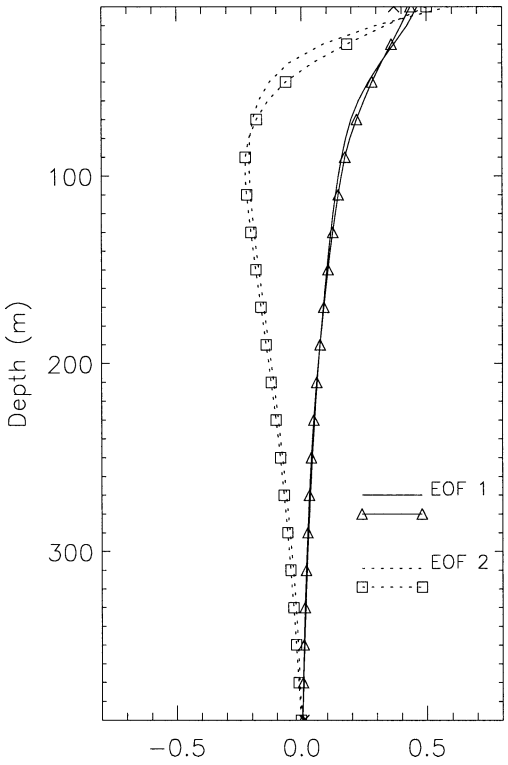

FIG. 5. The two leading dynamic height EOFs in the Balearic Sea: lines with symbols overplotted correspond to winter EOFS; lines alone correspond to summer EOFs.

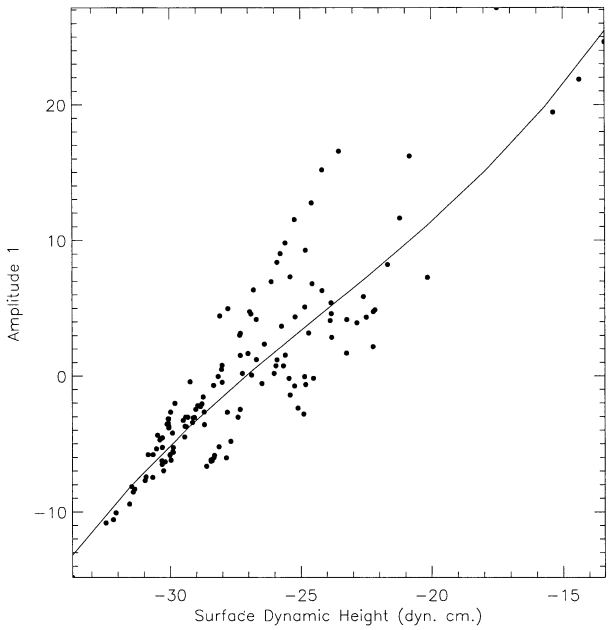

FIG. 6. Amplitude of the first EOF vs surface values of dynamic height in the Balearic Sea. The continuous line is a third-order polynomial least squares fit.

the EOFs simply provide the ''most common'' structures in terms of explained variance, it is possible to have different physical features contributing to the same EOF and vice versa. In our case, the first EOF does not change sign in the vertical, indicating that there is no change in direction of the flow over the whole water column associated with this mode. Instead, the second mode crosses the zero line at about 40 m, indicating that its contributions above and below this level will act in opposite sense when modulating the contribution of the first mode.

d. Results of the extrapolation methods

Once the EOFs were computed from the dependent data set, the three methods described in section 2 were tested for each of the 15 independent cruises in the following ways. 1) Dynamic height and specific volume cruise data were objectively analyzed at all levels, in order to obtain the field values on a regular grid. 2) EOF amplitudes were computed at every grid point from surface dynamic height and specific volume data, using Eqs. (2), (5), and (6), respectively for each method. 3) Dynamic height fields were extrapolated downward from the amplitudes estimated by each of the methods and the (common) EOFs. 4) Geostrophic velocity and transport were computed from DH fields. 5) Extrapolated and observed velocity fields were compared.

Before presenting the comparative results of the different methods, some further details on the application of the empirical reference method must be given. Figure 6 shows a plot of surface historical DH data versus the first EOF amplitude. The Pearson correlation for the least squares regression fit was 0.85, compared to the 0.96 obtained in Carnes et al. (1990). When a similar fit was attempted for higher EOF modes, the obtained correlation was very low. Thus, vertical extrapolations by the least squares reference methods were not improved by considering more than the first mode.

Figures 7a and 7b correspond to geostrophic velocity across a vertical section coincident with T/P track 70 for two particular cruises. The first cruise was carried out in July 1982 (hereafter Jul) and the second in May 1995 (hereafter May). The two cruises were chosen because they represent two different states of the Catalan front: very weak in Jul, with maximum velocities of about 10 cm s^{-1}, and stronger in May, with maximum speeds of up to 20 cm s^{-1}. Conversely, the Balearic Current is more intense in Jul than in May, in agreement with the climatological background.

Comparing the results produced by the different methods, it seems clear that the method that better reproduces the deep structure of the velocity field is the 2-EOF method, the least squares method being the worst. In order to quantify the goodness of the extrapolations, root mean square (rms) differences with respect to the observed fields were computed for each level over the selected domain (Fig. 1). With the aim of having an additional reference to evaluate the benefits of the extrapolation methods, we also computed the departure of

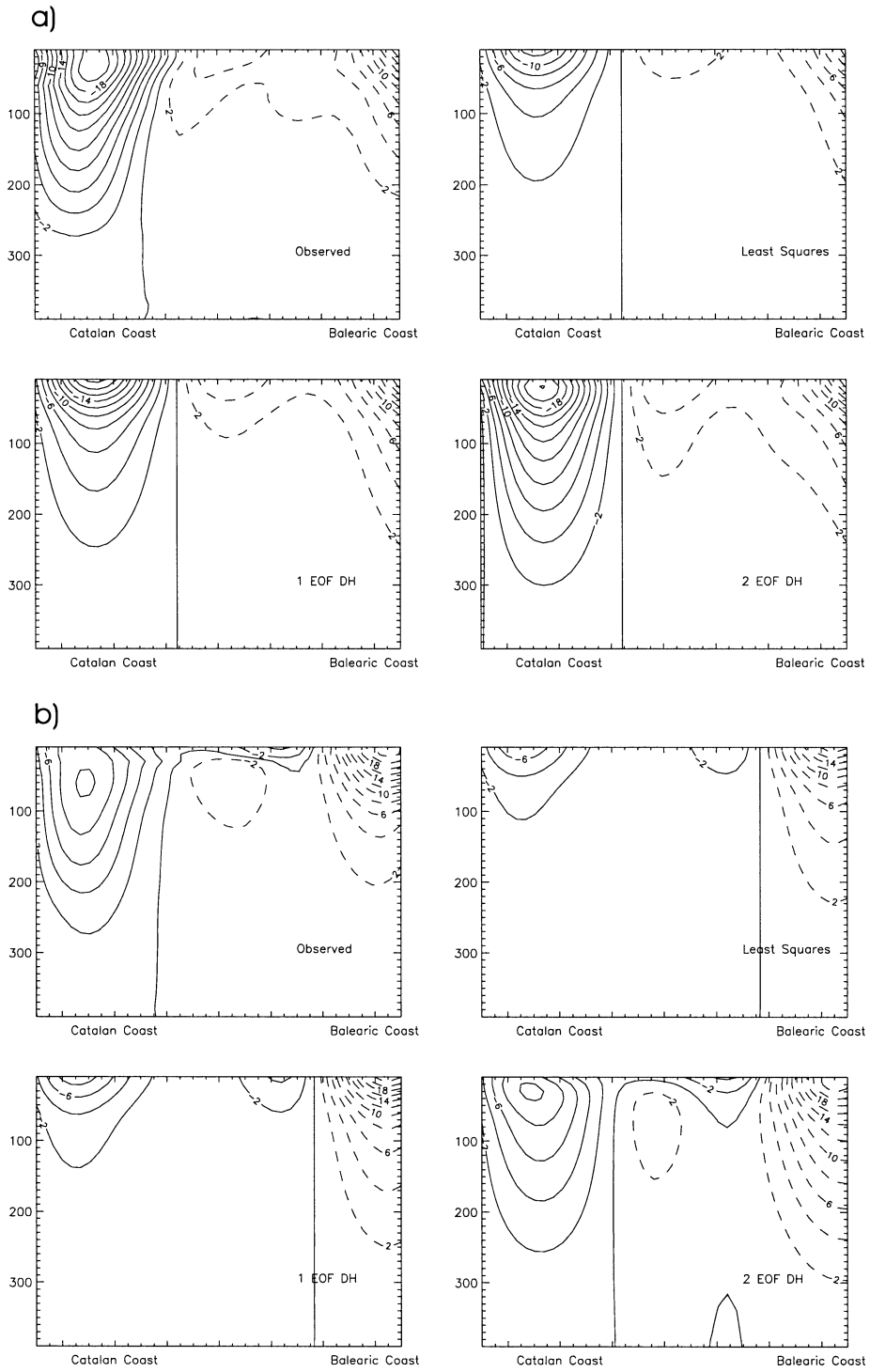

FIG. 7. (a) Cross-sectional geostrophic velocity over the vertical section underneath T/P track 70 for the May cruise: the four distributions correspond to the observed field and to the extrapolated fields produced by each of the three tested methods. (b) As in (a) but for the Jul cruise. [Units: cm s^{-1} with positive values (dashed) corresponding to a northeastward flow.]

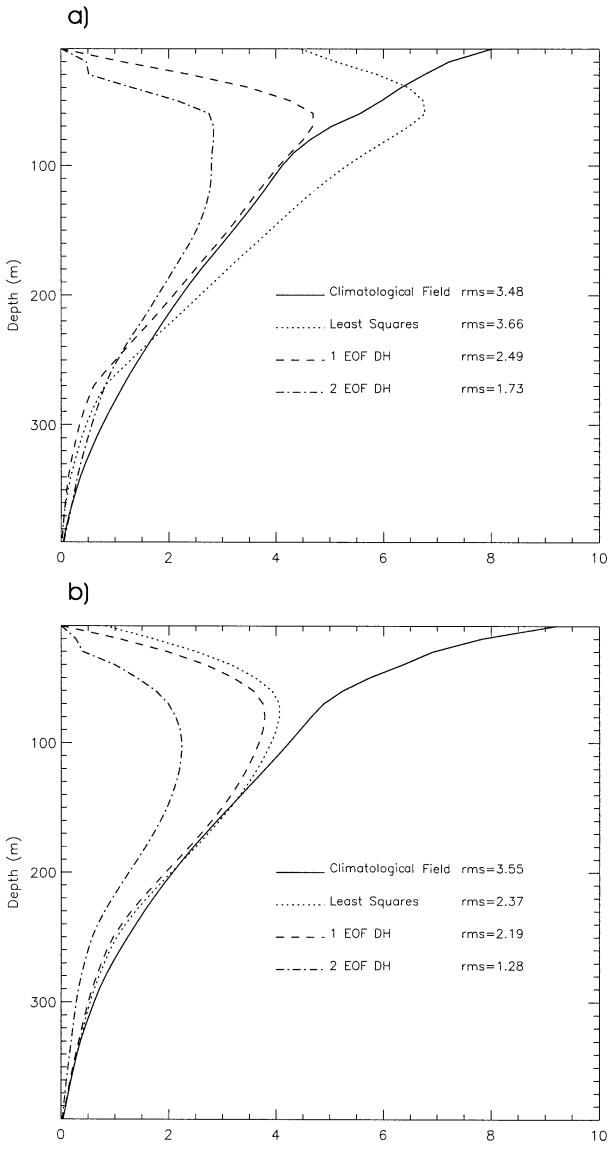

FIG. 8. Level statistics for the geostrophic velocity component perpendicular to T/P track 70. (a) Rms differences between the observed and interpolated fields produced by the different methods for the May cruise. (b) As in (a) but for the Jul cruise. (Units: cm s^{-1}.)

seasonal climatologies (computed from MODB data, in particular from the MED5 dataset) with respect to the observed fields. Figures 8a and 8b show the results for the two cruises, namely, rms differences for the cross-track geostrophic velocity component.

For the May cruise (Fig. 8a), the climatology rms differences are maximum at surface (8 cm s^{-1}), decreasing monotonically with depth. Instead, the least squares rms are maximum at about 50 m (6.7 cm s^{-1}), whereas at surface they are 4.5 cm s^{-1}. For the EOF methods, surface deviations from actual fields are exactly zero by definition, since the amplitudes are computed under this constraint. This is a big advantage compared to other methods in which some of the surface information is lost. For both EOF methods rms differences increase down to 50–100 m, approximately, where a reversal of the tendency is observed. Maximum rms values are about 4.7 cm s^{-1} for the 1-EOF method and 2.8 cm s^{-1} for the 2-EOF method. Similar results were obtained for the Jul cruise (Fig. 8b).

In order to have a single value representing the performance of each method, rms differences were averaged over all levels and quoted in Fig. 8. While the least squares method does not improve the trivial option of representing the fields by their seasonal climatology, the 2-EOF method reduces the differences between observed and climatological fields to less than a half. In terms of variance, the 2-EOF extrapolation explains more than 80% of the total. The performance of the 1-EOF method is in between the least squares fit and the 2-EOF method.

Investigating the spatial distribution of the misfits is almost as important as quantifying the benefits of every method. To do this, the geostrophic velocity component perpendicular to the T/P track, and the rms differences with respect to the observed field, were averaged over the 15 cruises representing the independent data. Figures 9 and 10 show the results at 30-m level over the area shown in Fig. 1. All the methods are able to capture the signal of the Catalan and Balearic fronts, locating the maximum currents in the right position. However, the magnitude of the velocities is clearly underestimated by the 1-EOF method (3 cm s^{-1} rms in the region of the Catalan front) and the least squares fitting (7 cm s^{-1} rms), whereas the 2-EOF method gets about the right magnitude (0.5 cm s^{-1} rms). Away from the frontal regions all methods give similar reasonable results. At a depth of 100 m (Figs. 11 and 12) the Balearic Current is weaker than the accuracy of the methods, but the Northern Current is still rather strong (8 cm s^{-1}). However, the latter is hardly detected by the 1-EOF and least squares methods. The 2-EOF method, despite working much better than the others, shows larger errors than at 30 m, as expected from previous results shown in Fig. 8.

It is therefore clear that including a second mode can not only reduce the mean errors, but also make their spatial distribution much more homogeneous. In other words, the second mode has proved to be essential to capture the frontal signal with an accuracy similar to the other regions of the domain. The reason for this feature is that higher-order modes not only account for progressively shorter vertical scales, but also for smaller horizontal scales, as it can be inferred from the patterns of the spatial distribution of amplitudes (Pedder and Gomis 1998). From the physical point of view, this would imply that the second mode contributes to explain the variability of the Balearic and Catalan fronts, which can be in terms of changes in the intensity and/or position of the associated currents, as well as, the possible formation of meanders.

Finally, from the vertical integration of the geostrophic velocity fields we obtained total geostrophic transport

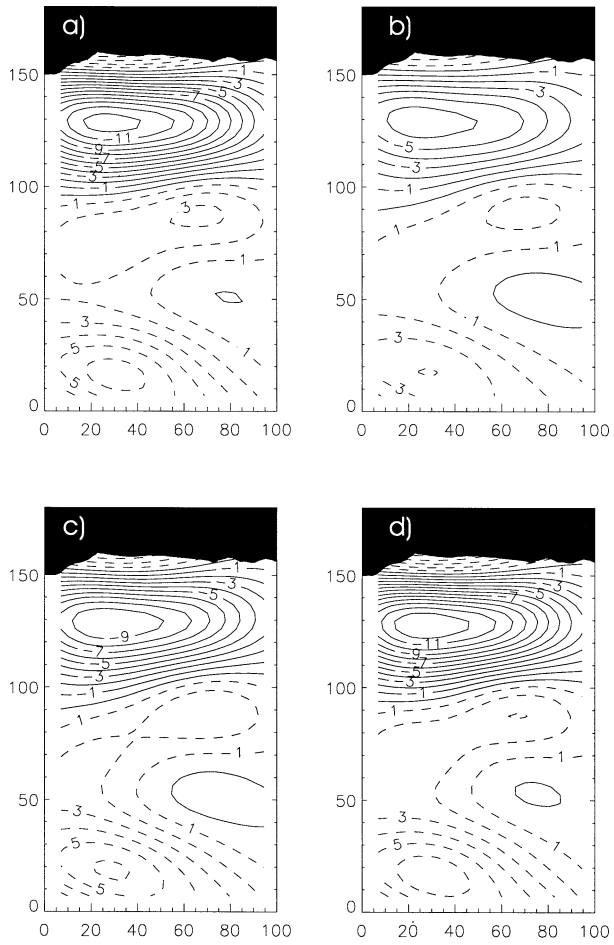

FIG. 9. Horizontal distribution at 30-m depth of the mean (averaged over the 15 independent cruises) geostrophic velocity component perpendicular to T/P track 70 for (a) the observed field, and the extrapolated fields produced by (b) the least squares fit, (c) the 1-EOF method, and (d) the 2-EOF method. [Units: cm s^{-1}, with positive values (dashed) corresponding to a northeastward flow.]

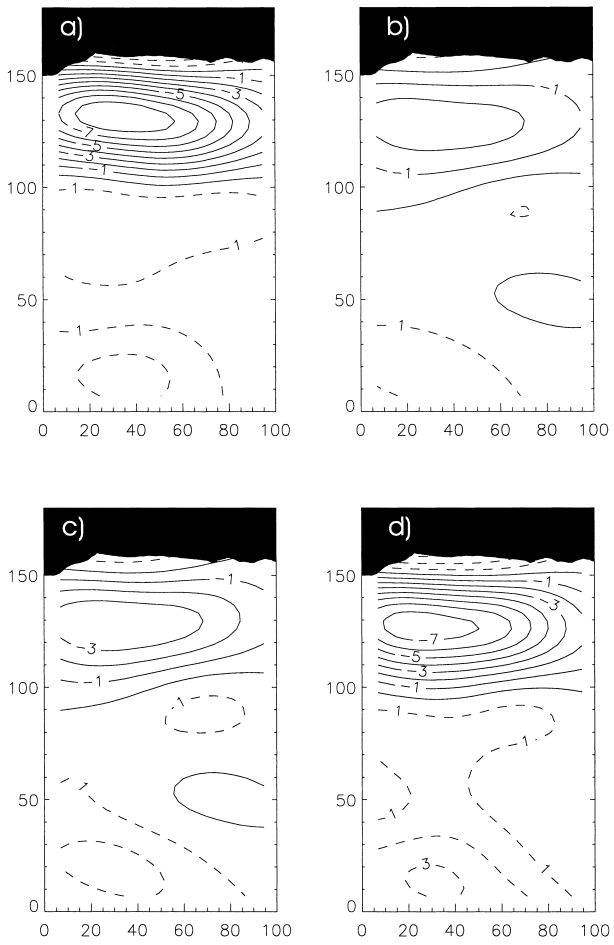

FIG. 11. As for Fig. 9, but at 100 m.

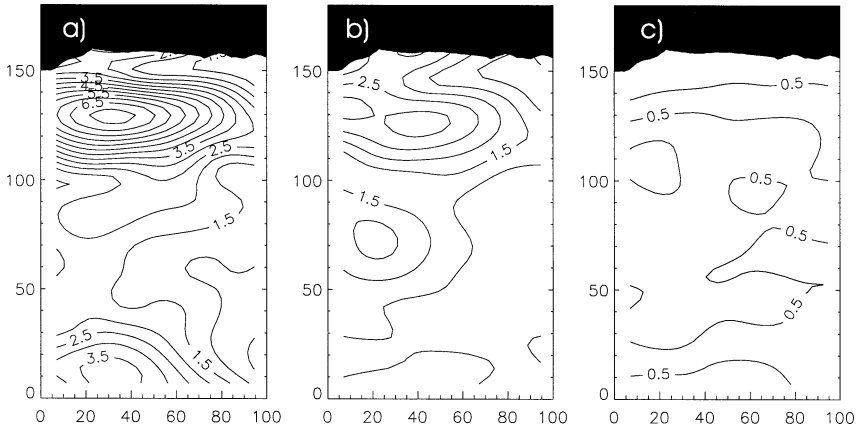

FIG. 10. Horizontal distribution at 30-m depth of the rms differences (averaged over the 15 independent cruises) between the observed geostrophic velocity component perpendicular to T/P track 70 and the extrapolated fields produced by (a) the least squares fit, (b) the 1-EOF method, and (c) the 2-EOF method. (Units: cm s^{-1}.)

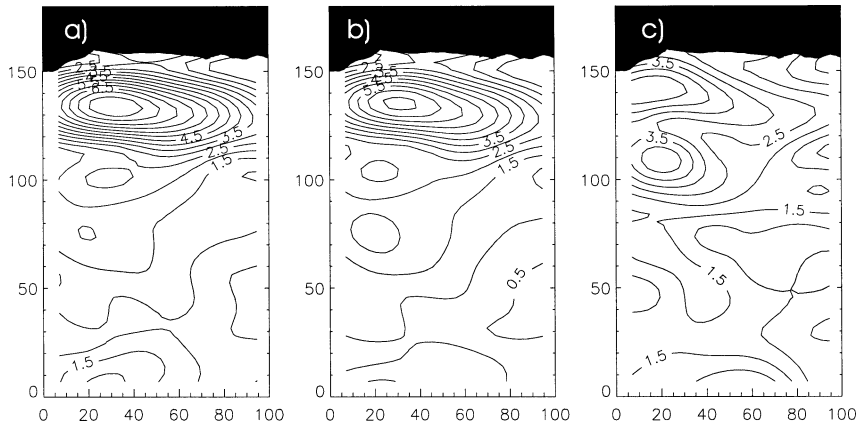

FIG. 12. As for Fig. 10, but at 100 m.

across the vertical section of the *T*/*P* track. Again, we computed rms differences not only between observed transport and the transport given by the different methods, but also between observed transport and the climatological transport (which is equivalent to the standard deviation of the anomaly field). The error variance of the different methods have been estimated as the squared rms differences between the estimated and observed transport normalized by the squared rms differences between the climatological and observed transport. A value of 1 (or 100% in terms of percentage) would be obtained for a method with a performance equivalent to substituting the observed field by the seasonal climatology.

The results, shown in Table 3, illustrate that the least squares method produces slightly worse results than climatology. On the other hand, the 1-EOF and 2-EOF methods reduce considerably the rms difference with respect to the climatology. In particular, the inclusion of the second EOF is crucial, since the explained fraction of the anomaly variance is almost 80% compared to the 35% obtained for the 1-EOF method. These statistical results are in good agreement with the previous results obtained for the two cruises, which indicate that the specific results shown before are representative of the whole dataset and are not exceptional cases.

4. Discussion and conclusions

The above results seem to indicate that the 2-EOF method can be a significant step forward in recovering the deep structure of the ocean from surface data. However, and precisely because of the significance of this step, the limitations of the method must also be clearly stated. Also the potential practical significance of the method deserves a detailed discussion.

a. On the intrinsic limitations of the method

First of all, any method based on EOFs relies on the underlying statistics. Hence, it should be ensured that the computed vertical modes are really representative of the region, and are uniform in space and time. Regarding time, this seems to be the case for our computations, since the small differences found between the seasonal EOFs suggest that temporal differences within each season should be even smaller. On the spatial side, the fact that the two first modes explain more than 97% of the field variance guarantees the capture of all significant spatial features, that is, higher modes, which usually represent local features, are negligible. Furthermore, since the historical data (profiles) used to compute the EOFs were from different locations and at different times, temporal and spatial variability in the region are assumed to be represented by the same vertical model structure. However, even under these optimal conditions, the method could be unable to properly recover unusual events—that is, those with a vertical structure very different from the statistics. These could be due for instance to wind storms which can distort the water column structure down to a few tens of meters, producing a mixed layer stronger than average. Or also,

TABLE 3. A measure of the error variance for the (geostrophic) transport estimated by the extrapolation methods. Figures correspond to squared rms differences between the estimated and observed transport normalized by the squared rms differences between the climatological and observed transport.

	Least squares		1 EOF DH		2 EOF DH	
Std dev (Sv)	Rms (Sv)	$\left(\frac{\text{rms}}{\text{std dev}}\right)^2$	Rms (Sv)	$\left(\frac{\text{rms}}{\text{std dev}}\right)^2$	Rms (Sv)	$\left(\frac{\text{rms}}{\text{std dev}}\right)^2$
0.34	0.35	113%	0.26	65%	0.15	21%

and probably more important, to the presence of significant anomalous features, such as the exceptional anticyclonic eddy described by Pascual et al. (2002) (this large amplitude eddy had a core of recent Atlantic Water and reversed the usual cyclonic circulation of the Balearic Sea for several months). Nevertheless, this limitation is intrinsic to any method relying on statistics and not of the particular method proposed in this work.

Regarding the way in which the amplitudes are estimated, it has already been stated that results would be strictly exact only when two vertical modes were enough to represent the total anomaly field (i.e., when the vertical structure of profiles can be reduced to two degrees of freedom). However, when the two leading modes account for 97% of the variability, as in the Balearic Sea, the estimation of amplitudes must be rather accurate, especially when it is compared with the accuracy of altimetric data (discussed later on).

The opposite case to the previous limitation would be when only one EOF is significant. This is for instance the case in the Alboran Sea (the westernmost basin of the Mediterranean Sea), where the first DH EOF accounts for 98% of the field variance (Pedder and Gomis 1998). The dynamics of this basin is characterized by the inflow of relatively light Atlantic Water. This enters the basin through the Strait of Gibraltar and then describes two almost permanent anticyclonic gyres, which occupy the first 200 m of the water column and exhibit velocities of up to 1.5 m s^{-1}. Below, the denser, resident Mediterranean Water is almost at rest. The structure of the two intense anticyclonic gyres resembles an equivalent barotropic ocean, with no tilting of the gyres in the vertical. In this particular scenario, the 1-EOF method and the least squares fit reported similar (or even slightly better) results than the 2-EOF method (not shown). This is not surprising, since when a single EOF is absolutely predominant, the contribution of the second can be attributed to noise.

b. On the operational application of the methods

A crucial question is to what extent the methods are feasible for an operational application. In that case, surface DH would have to be inferred from altimetric data, and surface SVAN from either a thermosalinograph installed on a ship of opportunity, or, in the future, from a combination of surface salinity provided by the SMOS satellite mission and sea surface temperature data from AVHRR satellite imagery.

Concerning the use of satellite data for inferring surface SVAN, the SMOS mission Font et al. (1999) is intended to provide, in the future, surface salinity observations, and could represent an important step forward in the understanding of the ocean. At present, only sea surface temperature (SST) measurements (from AVHRR) are accurate enough. The possibilities of inferring density from SST should then rely on historical correlations and would probably be regional dependent (in our region, a simple linear regression estimates density from temperature at 10 m with an error of ± 0.4 kg m^{-3}, not shown). But AVHRR measurements are only representative of the very surface layer (skin) and that could be a problem, especially in summer, when surface heating is maximum and the ''skin'' value is not representative of the water mass characteristics. On the other hand, there is the additional limitation of cloud cover. It should be then tested whether these handicaps cancel out or not the benefits of including a second mode in the extrapolation with respect to using only the first leading EOF estimated from altimetry.

Another option could be the use of a thermosalinograph installed on a ship of opportunity. These devices measure surface (at about 5-m depth) temperature and salinity, can be installed with a reasonable cost, and can work unattended, so that they would constitute an alternative to the present common practice of launching XBTs from ships of opportunity (in fact, some thermosalinographs have already been installed in the Japanese fishing fleet; M. Filella 2002, personal communication). The handicap of using ships of opportunity is that their routes are usually not the same as the altimeter tracks. A possibility could be to work with interpolated altimetry maps (with the values closer to the ship track), which are nowadays a standard product (MGC-B, version 2; AVISO 1996).

Regarding the inference of dynamic height from sea level (measured by altimeters) they are obviously not equivalent: dynamic height captures all baroclinic processes above a reference level of specific pressure, while sea level also includes the motions below this reference level, as well as barotropic processes. Moreover, the T/P orbit accuracy is of 2 cm (e.g., Tapley et al. 1994), which is a considerable fraction of the field variance in some regions as the Mediterranean Sea, where the topography signal is small, of the order of 10 cm (Larnicol et al. 1995).

Finally, altimetric measurements are relative to the geoid (an equipotential surface of the earth gravity field to which a motionless ocean surface would conform). The main limitation of altimetry is that the shape of the geoid is not sufficiently known at scales less than about 2500 km (from which the geoid models are accurate enough; Nerem et al. 1994). Therefore, it is presently impossible to derive accurate absolute currents from altimetry alone.

Some attempts to circumvent the geoid problem have been made in the sense of using ''synthetic'' geoids determined from model simulations of the mean current (Glenn et al. 1991) or, more successfully, from combining altimetric and hydrographic data along satellite tracks (Laing and Challenor 1999). In the absence of in situ data coincident with satellite altimeter tracks, an alternative approach is to add a climatological mean dynamic height field (derived from historical hydrographic data) to two-dimensional analyses of altimeter-derived sea level anomalies (e.g., Hernández et al. 1995). This allows having collocated, simultaneous hy-

drographic and satellite data, but at the expenses of reducing the spatial resolution, which can be crucial in regions characterized by significant mesoscale variability.

In the Mediterranean, most altimetry studies have concentrated on describing the temporal variability of sea level using the so-called sea level anomaly (SLA), obtained by subtracting the mean sea level (the geoid and the elevation due to mean currents) from the absolute sea surface elevation over a reference ellipsoid (e.g., Larnicol et al. 1995; Ayoub et al. 1998; Iudicone et al. 1998). No direct comparison between hydrography and altimetry had been performed until the Altimeter/Synoptic Mesoscale Planckton Experiment. Within this project, Buongiorno Nardelli et al. (1999) performed in situ measurements simultaneous to the passage of T/P and *ERS-2* over selected tracks in the central and eastern Sicily Channel. Because permanent currents are not very important in that region, SLA were directly compared against in situ data.

In the Balearic Sea, a detailed work on the comparisons between altimetry and hydrography is in process (Isern-Fontanet et al. 2001, personal communication). This study will use data collected during the GPS Radar Altimeter Calibration (GRAC) project and will examine all the possible error sources of missmatches between DH and sea level. We can anticipate that the differences are not due to a missing barotropic component or to a wrong reference level. Instead, the main contributions are likely to come from the limited accuracy of present altimeters and from the fact that the mean sea level removed from the altimetric data contain an important part (the steady currents) of the total signal. These contributions are both likely to reduce in the near future, when longer data series are available and with the better accuracy of the new generation of altimeters (Jason and ENVISAT).

Summarizing, the proposed method can be envisaged as a useful tool for an operational application, with very low computational cost. By combining routine altimetric data with surface density data from ships of opportunity (e.g., from thermosalinographs installed in ferries running approximately along satellite tracks) it would be possible to recover the structure of the velocity field underneath the track with a substantial improvement over previous methods. This can be crucial for the monitoring of the Balearic Sea, since T/P track 70 runs along the northern boundary of the basin and it is almost perpendicular to the main currents entering and exiting the basin. Future studies should confirm the feasibility of the operational implementation of the methods as well as the application to other parts of the ocean.

Acknowledgments. We wish to express our gratitude to the MAST Supporting Initiatives MODB and MEDATLAS, which have been crucial to this work. We are thankful to J. Salat and M. Massó, who provided cruise data not included in the existing databases (the cruises were funded by the Spanish Comisión Interministerial de Ciencia y Tecnología under Contracts AMB-93-0728 and AMB-94-0853, respectively). Ananda Pascual holds a doctoral fellowship from the Universitat de les Illes Balears. Finally, we want to thank Dr. Robert L. Haney for his useful suggestions on the contents and presentation of the work.

REFERENCES

AVISO, 1996: User handbook for merged TOPEX/POSEIDON products. 3d ed. AVI-NT-02-101-CN, Toulouse, France, 196 pp.

Ayoub, N., P.-Y. Le Traon, and P. de Mey, 1998: A description of the Mediterranean surface variable circulation from combined ERS-1 and Topex/Poseidon altimetric data. *J. Mar. Syst.,* **18** (1–3), 3–40.

Bethoux, J. P., L. Prieur, and J. H. Bong, 1988: Le courant Ligure au large de Nice. *Oceanol. Acta,* **9,** 59–67.

Boyd, J. D., E. P. Kennelly, and P. Pistek, 1994: Estimation of EOF expansion coefficients from incomplete data. *Deep-Sea Res.,* **94,** 1479–1488.

Brasseur, P., J.-M. Brankart, R. Schoenauen, and J.-M. Beckers, 1996: Seasonal temperature and salinity fields in the Mediterranean Sea: Climatological analyses of an historical data set. *Deep-Sea Res.,* **43,** 159–192.

Bratseth, A. M., 1986: Statistical interpolation by means of successive correction. *Tellus,* **38A,** 439–447.

Buongiorno Nardelli, B., R. Santoleri, D. Iudicone, S. Zoffoli, and S. Marullo, 1999: Altimetric signal and three-dimensional structure of the sea in the Channel of Sicily. *J. Geophys. Res.,* **104,** 20 585–20 603.

Carnes, M. R., J. L. Mitchell, and P. W. DeWitt, 1990: Synthetic temperature profiles derived from GEOSAT altimetry: Comparison with air-dropped expendable bathythermograph profiles. *J. Geophys. Res.,* **95,** 17 979–17 992.

Carton, J. A., and E. J. Katz, 1990: Estimates of the zonal slope and seasonal transport of the Atlantic North Equatorial Countercurrent. *J. Geophys. Res.,* **95,** 3091–3100.

Castellón, A., J. Font, and E. García-Ladona, 1990: The Liguro–Provençal–Catalan current (NW Mediterranean) observed by Doppler profiling in the Balearic Sea. *Sci. Mar.,* **54,** 269–276.

de Mey, P., and A. R. Robinson, 1987: Assimilation of altimeter eddy fields in a limited-area quasi-geostrophic model. *J. Phys. Oceanogr.,* **17,** 2280–2293.

Ezer, T., and G. L. Mellor, 1994: Continuous assimilation of GEOSAT altimeter data into a three-dimensional primitive equation Gulf Stream model. *J. Phys. Oceanogr.,* **24,** 832–847.

Fichaut, M., E. Balopoulos, L. Baudet, H. Dooley, M.-J. Garcia-Fernandez, A. Iona, D. Jourdan, and C. Maillard, 1997: A common protocol to assemble a coherent database from distributed heterogeneous data sets: The MEDATLAS database example. Proc. MAST Workshop on Project Data Management, Ispra, Italy, MAST, 1–18.

Font, J., 1990: A comparison of seasonal winds with currents on the continental slope of the Catalan Sea (northwestern Mediterranean). *J. Geophys. Res.,* **95,** 1537–1545.

——, J. Salat, and J. Tintoré, 1988: Permanent features of the circulation in the Catalan Sea. *Oceanol. Acta,* **9,** 51–57.

——, E. García-Ladona, and E. G. Gorriz, 1995: The seasonality of mesoscale motion in the Northern Current of the western Mediterranean: Several years of evidence. *Oceanol. Acta,* **18,** 207–219.

——, Y. Kerr, M. Srokosz, J. Etcheto, G. Lagerloef, and P. Waldteufel, 1999: SMOS mission: Observing ocean surface salinity from space. *Proc. Int. Conf. on the Ocean Observing System for Climate,* St. Raphael, France, CNES, OOPC, CLIVAR/UOP.

Gavart, M., and P. de Mey, 1997: Isopycnal EOFs in the Azores

Current region: A statistical tool for dynamical analysis and data assimilation. *J. Phys. Oceanogr.,* **27,** 2146–2157.

——, ——, and G. Caniaux, 1999: Assimilation of satellite altimeter data in a primitive-equation model of the Azores–Madeira region. *Dyn. Atmos. Oceans,* **29,** 217–254.

Gilson, J., D. Roemmich, B. Cornuelle, and L.-L. Fu, 1998: Relationship of TOPEX/POSEIDON altimetric height to steric height and circulation in the North Pacific. *J. Geophys. Res.,* **103,** 27 947–27 965.

Glenn, S. M., D. L. Porter, and A. R. Robinson, 1991: A synthetic geoid validation of GEOSAT mesoscale dynamic topography in the Gulf Stream region. *J. Geophys. Res.,* **96,** 7145–7166.

Haney, R. L., R. A. Hale, and C. A. Collins, 1995: Estimating subpycnocline density fluctuations in the California Current region from upper ocean observations. *J. Atmos. Oceanic Technol.,* **12,** 550–566.

Hernández, F., P.-Y. Le Traon, and R. Morrow, 1995: Mapping mesoscale variability of the Azores Current using TOPEX/POSEIDON and ERS-1 altimetry, together with hydrographic and Lagrangian measurements. *J. Geophys. Res.,* **100,** 24 995–25 006.

Hurlburt, H. E., 1984: The potential for ocean prediction and the role of altimeter data. *Mar. Geod.,* **8,** 17–66.

Imawaki, S., H. Uchida, H. Ichikawa, M. Fukasawa, S. Umatani, and ASUKA Group, 1997: Time series of the Kuroship Transport derived from field observations and altimetry data. *International WOCE Newsletter,* No. 25, WOCE International Office, Southampton, United Kingdom, 15–18.

Iudicone, D., R. Santoleri, S. Marullo, and P. Gerosa, 1998: Sea level variability and surface eddy statistics in the Mediterranean Sea from TOPEX/POSEIDON data. *J. Geophys. Res.,* **103,** 2995–3011.

Laing, A. K., and P. G. Challenor, 1999: Estimation of mean dynamic height from altimeter profiles and hydrography. *J. Atmos. Oceanic Technol.,* **16,** 1873–1879.

Larnicol, G., P. Y. Le Traon, N. Ayoub, and P. de Mey, 1995: Mean sea level and surface circulation variability of the Mediterranean Sea from 2 years of TOPEX/POSEIDON altimetry. *J. Geophys. Res.,* **100,** 25 163–25 177.

Leuliette, E. W., and J. M. Wahr, 1999: Coupled pattern analysis of sea surface temperature and TOPEX/Poseidon sea surface height. *J. Phys. Oceanogr.,* **29,** 599–611.

López García, M. J., C. Millot, J. Font, and E. García-Ladona, 1994: Surface circulation variability in the Balearic Basin. *J. Geophys. Res.,* **99,** 3285–3296.

Mellor, G. L., and T. Ezer, 1991: A Gulf Stream model and an altimetry assimilation scheme. *J. Geophys. Res.,* **96,** 8779–8795.

Nerem, R. S., and Coauthors, 1994: Gravity model development for TOPEX/POSEIDON: Joint gravity models 1 and 2. *J. Geophys. Res.,* **99,** 24 421–24 447.

Oschlies, A., and J. Willebrand, 1996: Assimilation of GEOSAT altimeter data into an eddy-resolving primitive equation model of the North Atlantic Ocean. *J. Geophys. Res.,* **101,** 14 175–14 190.

Overland, J. E., and R. W. Preisendorfer, 1982: A significance test for principal components applied to a cyclone climatology. *Mon. Wea. Rev.,* **110,** 1–4.

Pascual, A., B. Buongiorno Nardelli, G. Larnicol, M. Emelianov, and D. Gomis, 2002: A case of an intense anticyclonic eddy in the Balearic Sea (western Mediterranean). *J. Geophys. Res.,* **107** (C11), 3183, doi:10.1029/2001JC000913.

Pedder, M. A., 1993: Interpolation and filtering of spatial observations using successive corrections and Gaussian filters. *Mon. Wea. Rev.,* **121,** 2889–2902.

——, and D. Gomis, 1998: Application of EOF analysis to the spatial estimation of circulation features in the ocean sampled by high-resolution CTD samplings. *J. Atmos. Oceanic Technol.,* **15,** 959–978.

Pinot, J. M., J. Tintoré, and D. Gomis, 1995: Multivariate objective analysis of the surface circulation in the Balearic Sea. *Progress in Oceanography,* Vol. 36, Pergamon, 343–376.

Tapley, B. D., and Coauthors, 1994: Precision orbit determination for TOPEX/POSEIDON. *J. Geophys. Res.,* **99,** 24 383–24 404.

Tintoré, J., D. P. Wang, and La Violette, 1990: Eddies and thermohaline intrusions of the shelf/slope front off northeast Spain. *J. Geophys. Res.,* **95,** 1627–1633.